Sensors and Actuators B 191 (2014) 659–665

Contents lists available at ScienceDirect

Sensors and Actuators B: Chemical

journal homepage: www.elsevier.com/locate/snb

Sensitive ethanol sensors fabricated from p-type $La_{0.7}Sr_{0.3}FeO_3$ nanoparticles and n-type SnO_2 nanofibers

Qi Qi[a], Jun Zhao[a], Rui-Fei Xuan[a,c], Pei-Pei Wang[a], Liang-Liang Feng[a], Li-Jing Zhou[a], De-Jun Wang[a,b], Guo-Dong Li[a,*]

[a] State Key Lab of Inorganic Synthesis & Preparative Chemistry, College of Chemistry, Jilin University, Changchun 130012, PR China
[b] Department of Chemistry, Tsinghua University, Beijing 100086, PR China
[c] College of Materials Science and Engineering, China University of Mining and Technology, Xuzhou 221116, PR China

ARTICLE INFO

Article history:
Received 16 July 2013
Received in revised form
19 September 2013
Accepted 7 October 2013
Available online 19 October 2013

Keywords:
$La_{0.7}Sr_{0.3}FeO_3$ nanoparticles
SnO_2 nanofibers
Electrospinning
Semiconductors
Gas sensors

ABSTRACT

$La_{0.7}Sr_{0.3}FeO_3$ nanoparticles are prepared by a citrate method, and SnO_2 nanofibers are synthesized via an electrospinning process. In order to improve the sensing performance, $La_{0.7}Sr_{0.3}FeO_3$ nanoparticles are coated on the surface of SnO_2 nanofibers. The materials are characterized by X-ray diffraction (XRD), scanning electron microscopy (SEM), transmission electron microscopy (TEM), and energy dispersive spectroscopy (EDS). Three sensors are fabricated from $La_{0.7}Sr_{0.3}FeO_3$ coated SnO_2 nanofibers with different coating times. And the sensors with only $La_{0.7}Sr_{0.3}FeO_3$ nanoparticles and SnO_2 nanofibers are also fabricated for comparison. The sensors are exposed to ethanol with various concentrations and operating temperatures, and sensor performances are calculated and evaluated by a sensing analysis system automatically. It is clear that the sensors based on SnO_2 nanofibers with four times of $La_{0.7}Sr_{0.3}FeO_3$ coating (L_4SnO_2 sensors) own the highest response of 28–1 ppm ethanol, which is 5 times larger than that of SnO_2 nanofiber sensors and 8 times greater than that of $La_{0.7}Sr_{0.3}FeO_3$ nanoparticle sensors. Moreover, fast response and recovery, good selectivity, anti-humidity, and high stability of L_4SnO_2 sensors are obtained herein. To understand the improved performance of L_4SnO_2 sensor, the sensing mechanism is discussed.

© 2013 Elsevier B.V. All rights reserved.

1. Introduction

SnO_2 is a kind of important sensing materials for chemical sensors due to its significant surface reactivity with both reducing (CO, C_2H_2, CH_4, and H_2) and oxidizing gases (Cl_2, O_2, NO_X, and SO_2) [1,2]. Among those sensors based on SnO_2, one-dimensional (1D) SnO_2 nanostructures have called great attention for their gas response as well as chemical stability [3]. In particular, a series of 1D SnO_2 nanostructures, such as nanorods [4], nanotubes [5], nanofibers [6], nanowires [7], and nanobelts [8] have been successfully synthesized and applied to gas sensing. Many unique gas sensing properties were reported based on 1D SnO_2 nanostructures [9]. And recent investigations also revealed that the sensing performance of these 1D SnO_2 nanostructures could be further enhanced by doping other atoms [10].

In order to improve the sensing properties of SnO_2-based gas sensors, three kinds of doping strategies are developed. Firstly, modifying the surface of sensing materials by noble metals (Au, Pt or Pd) [11–13] or rare earth elements (La, Y and Ce) is a popular route [14]. Correspondingly, electronic and chemical sensitizations have been widely applied in these cases [15]. Secondly, forming composites with other n-type semiconductors such as ZnO [16], In_2O_3 [17] and TiO_2 [18] can also enhance the sensing response and reacting speeds. Using p-type semiconductors, such as CuO [19] or NiO [20], to modify SnO_2 is another critical approach. When these p–n composites are exposed to a target gas, the chemical species to be detected in the atmosphere can be absorbed on the interface of the p–n contacts [21], and leading to the amplified electrical resistance changes of the sensors. This p–n heterojunction concept was introduced in 1979 and has been widely applied in humidity sensors, liquid sensors and gas sensors [22].

Herein, we present sensitive ethanol sensors fabricated from p-type $La_{0.7}Sr_{0.3}FeO_3$ nanoparticles and n-type SnO_2 nanofibers. $La_{0.7}Sr_{0.3}FeO_3$ is a typical ABO_3 type material which shows excellent selectivity and good stability to reducing gases [23]. SnO_2 nanofibers are known for their high response and short response and recovery times [24–26]. Both of these two types of materials are sensitive to ethanol. While, the composite materials show improved and excellent ethanol sensing properties, which are mainly due to the p–n contacts on sensor surface.

* Corresponding author. Tel.: +86 431 85168318; fax: +86 431 85168624.
E-mail addresses: lifind@21cn.com, lgd@jlu.edu.cn (G.-D. Li).

0925-4005/$ – see front matter © 2013 Elsevier B.V. All rights reserved.
http://dx.doi.org/10.1016/j.snb.2013.10.035

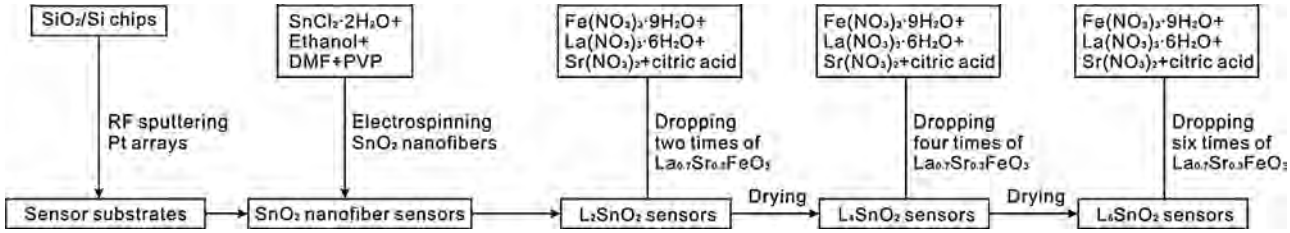

Fig. 1. Schematic diagram of the sensor fabrication.

2. Experimental

2.1. Synthesis of materials and fabrication of sensors

All chemicals (analytical grade reagents) were purchased from Beijing Chemicals Co. Ltd. and used as received without further purification. Deionized water with a resistivity of 18.2 MΩ cm^{-1} was used in all experiments. Nanocrystalline $La_{0.7}Sr_{0.3}FeO_3$ was prepared by a citrate method [27]. According to the formula $La_{0.7}Sr_{0.3}FeO_3$, 0.7 mmol of $La(NO_3)_3{\cdot}6H_2O$, 0.3 mmol of $Sr(NO_3)_2$ and 1.0 mmol of $Fe(NO_3)_3{\cdot}9H_2O$ were dissolved into 80 mL of deionized water, and then 15 mg of citric acid was dropped into the mixture. Then, the mixture was heated at 80 °C and stirred for 2 h to obtain a homogeneous precursory sol of $La_{0.7}Sr_{0.3}FeO_3$. SnO_2 nanofibers were synthesized via a simple electrospinning method [28]. Typically, 0.4 g of $SnCl_2{\cdot}2H_2O$ was mixed with 4.42 g of N,N-dimethylformamide (DMF) and 4.42 g of ethanol in a glove box under vigorous stirring for 6 h. Subsequently, 0.8 g of poly(vinyl pyrrolidone) (PVP, Mw = 1,300,000) was added to this solution and stirred for another 6 h. The obtained slurry was delivered to a hypodermic syringe at a constant flow rate of 1.0 mL/h, and then electrospun by applying 10 kV at an electrode distance of 20 cm. A piece of aluminum foil was used as the cathode and several sensor substrates were placed on it.

Sensor substrates were fabricated by radio-frequency (RF) sputtering method, and Pt arrays were deposited on SiO_2/Si chips as signal and heating electrodes. The thickness of SiO_2 layer and Pt array were about 300 and 100 nm, respectively. The sensor length and width were 3 and 2 mm. The precursor solution was directly electrospun on the sensor substrates. After electrospinning for 4 h, the sensor substrates with precursory nanofibers were obtained. Then, the sol of $La_{0.7}Sr_{0.3}FeO_3$ will be dropped on them for several times. After each step, the substrate was dried at 100 °C for 2 h before the next step. Finally, the $La_{0.7}Sr_{0.3}FeO_3$-coated SnO_2 sensors were calcined at 600 °C for 5 h in air, and followed by annealing at 300 °C for 10 min in nitrogen atmosphere.

Three sensing materials with different dropping times (2, 4, and 6) were prepared, and the corresponding sensors are denoted as L_2SnO_2 sensors, L_4SnO_2 sensors, and L_6SnO_2 sensors in this paper. Sensors with only $La_{0.7}Sr_{0.3}FeO_3$ nanoparticles and SnO_2 nanofibers were also prepared for comparison. Fig. 1 shows a schematic diagram of the methodology used for sensor fabrication.

2.2. Characterization of materials and measurement of sensors

X-ray diffraction (XRD) analysis was conducted on a Rigaku D/Max 2550 X-ray diffractometer (XRD) with Cu Kα radiation (λ = 1.5418 Å). Scanning electron microscopy (SEM) images and energy dispersive spectroscopy (EDS) spectra were performed on a JEOL JSM 6700F. Transmission electron microscope (TEM) images were obtained on a FEI Tecnai G2S-Twin with a field emission gun operating at 200 kV.

Sensing measurement was performed on a CGS-8 (Chemical Gas Sensor-8) intelligent gas sensing analysis system [29], as shown in Fig. 2(a) and (b) (Beijing Elite Tech Co., Ltd., China). This system could provide various operating currents to control the sensor temperature (measured by a Testo 845 infrared thermometer (TESTO AG, Germany)). All of the sensors were pre-heated at different operating temperatures for 30 min. When the resistances of the sensors were stable, saturated target gas was injected into the test chamber (20 L in volume) by a micro-injector through a rubber plug. The saturated target gas was mixed with air by two fans in the analysis system. After the sensor resistances reached new constant values, the test chamber was opened to recover the sensors in air. The humidity and temperature of testing environment are 25% RH and 20 °C, respectively.

The sensor response (R) was designated as $R = Ra/Rg$, where Ra was the sensor resistance in air (base resistance) and Rg was that in a mixture of target gas and air. The time taken by the sensor resistance to change from Ra to $Ra - 90\% \times (Ra - Rg)$ was defined as response time when the target gas was introduced to the sensor, and the time taken from Rg to $Rg + 90\% \times (Ra - Rg)$ was defined as recovery time when the ambience was replaced by air [20].

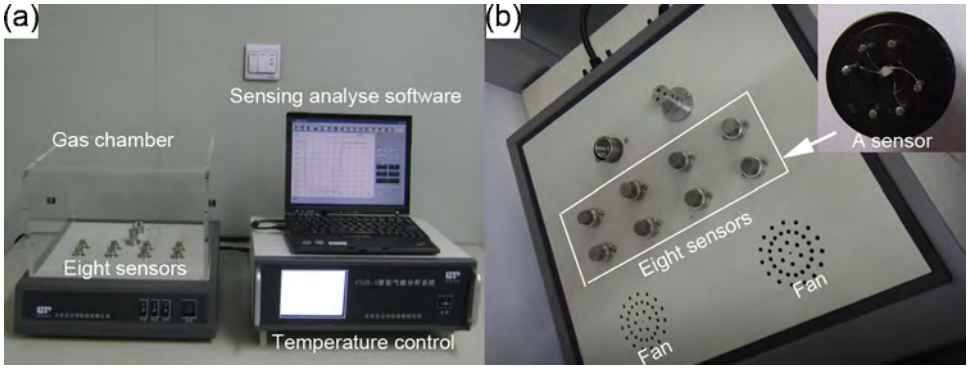

Fig. 2. Photographs of (a) a CGS-8 intelligent gas sensing analysis system and (b) the gas chamber with eight sensors in it.

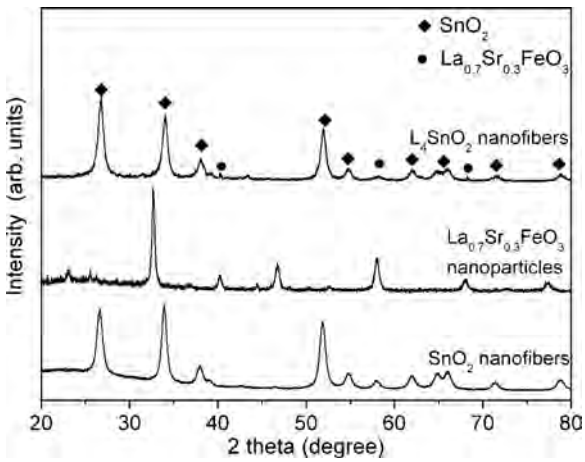

Fig. 3. XRD patterns of SnO_2 nanofibers, $La_{0.7}Sr_{0.3}FeO_3$ nanoparticles, and L_4SnO_2 nanofibers.

3. Results and discussion

The XRD patterns of SnO_2 nanofibers, $La_{0.7}Sr_{0.3}FeO_3$ nanoparticles, and L_4SnO_2 nanofibers are shown in Fig. 3. Diffractions from SnO_2 nanofibers, $La_{0.7}Sr_{0.3}FeO_3$ nanoparticles can be well indexed to rutile type of SnO_2 and cubic structure of $La_{0.7}Sr_{0.3}FeO_3$, respectively. And the diffraction peaks corresponding to $La_{0.7}Sr_{0.3}FeO_3$ are also observed in the XRD pattern of L_4SnO_2 nanofibers. While the location of the diffraction peaks of SnO_2 in L_4SnO_2 nanofibers is nearly the same as that of pure SnO_2. The grain sizes of SnO_2 in SnO_2 nanofibers and L_4SnO_2 nanofibers are very close, which are estimated to be about 21 and 20 nm according to Scherrer formula [11]. The retained diffraction peaks and grain sizes suggest that crystal $La_{0.7}Sr_{0.3}FeO_3$ deposits on the surface of SnO_2 nanofibers instead of forming solid solution. It may be resulted from the different thermal decomposition behaviors between $SnCl_2$/PVP composite nanofibers and $La(NO_3)_3$/$Sr(NO_3)_2$/$Fe(NO_3)_3$/citric acid precursors. Similar phenomena are found in other reports [30,31], and the phase separation in this process will lead to the formation of heterostructures in the final materials.

Fig. 4(a–f) shows the SEM images of the $La_{0.7}Sr_{0.3}FeO_3$ nanoparticles, SnO_2 nanofibers, L_2SnO_2 nanofibers, L_4SnO_2 nanofibers, L_6SnO_2 nanofibers, and the magnified L_4SnO_2 nanofibers, respectively. In Fig. 4(a), $La_{0.7}Sr_{0.3}FeO_3$ nanoparticles with an average diameter around 20 nm are compactly agglomerated, which is not beneficial for gas to fast penetrate into the sensing layer. While, in Fig. 4(b), the SnO_2 nanofibers are collected as randomly oriented structures with an average diameter about 80 nm and lengths up to several microns. The insert TEM image reveals that the nanofibers are consisted of nanoparticles (the average diameter is about 15 nm). As shown in Fig. 4(c–e), more and more $La_{0.7}Sr_{0.3}FeO_3$ nanoparticles are gradually deposited on the surface of SnO_2 nanofibers with the increase of the dropping times. From the magnified L_4SnO_2 nanofibers of Fig. 4(f), it is clear that $La_{0.7}Sr_{0.3}FeO_3$ nanoparticles packed tightly on the surface of SnO_2 nanofibers.

Corresponding EDS spectra from the as-prepared pure SnO_2, L_2SnO_2, L_4SnO_2 and L_6SnO_2 nanofibers are shown in Fig. 5. The EDS results reveal that the synthesized nanofibers are composed of Sn, O, Fe, La and Sr. Fig. 5(a) shows the presence of only Sn and O in about 1:2 mole ratio (within experimental error) and the three characteristic Sn peaks are at about 3.46, 3.68 and 3.92 keV [32]. The atomic percentage of $La_{0.7}Sr_{0.3}FeO_3$ in the as-synthesized products is found to about 1.5 at%, 3.7 at% and 11.4 at% for L_2SnO_2, L_4SnO_2 and L_6SnO_2 nanofibers, respectively (Fig. 5(b–d)). The peaks of C and Al are derived from the conducting resin and Al platform during the measurement.

All the sensors are exposed to 1 ppm ethanol at different operating temperatures (240–340 °C) to determine the optimum working condition. As shown in Fig. 6, the responses of the five sensors to 1 ppm ethanol vapor increased with the increased operating temperatures and reached maximum values. The temperatures corresponding to the maximum responses for SnO_2 sensors, L_2SnO_2 sensors, L_4SnO_2 sensors, and L_6SnO_2 sensors are 300 °C, and for

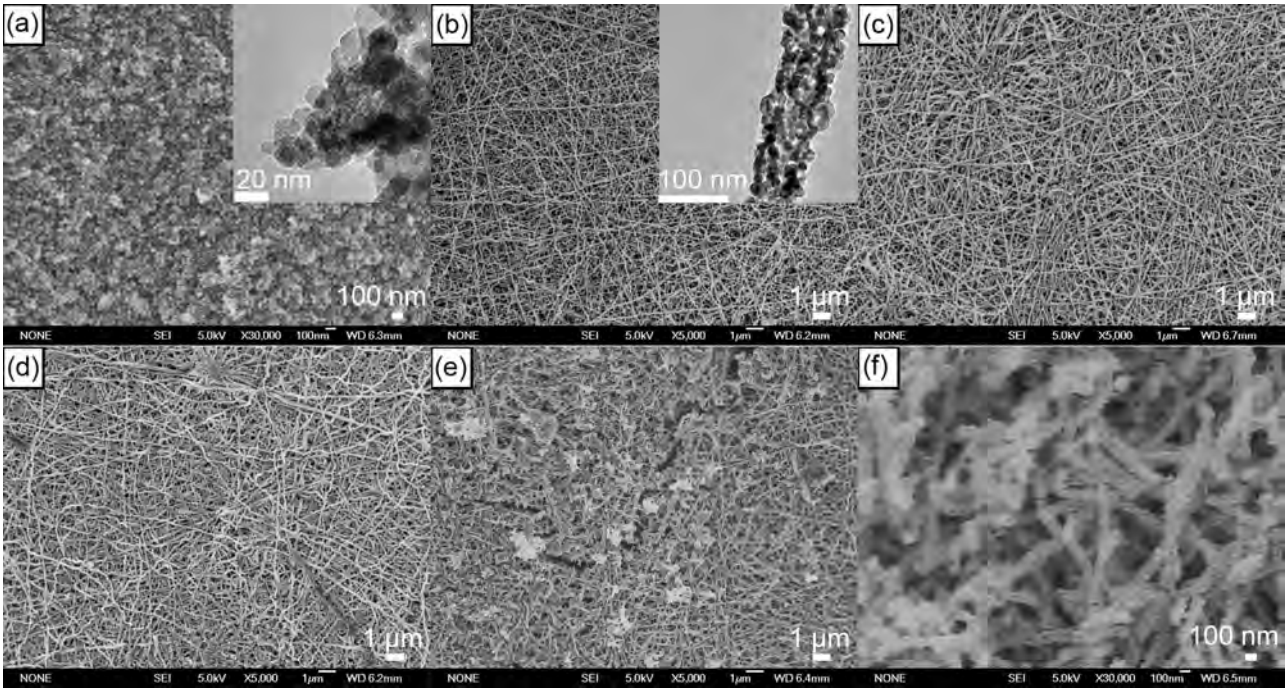

Fig. 4. SEM images of (a) $La_{0.7}Sr_{0.3}FeO_3$ nanoparticles, (b) SnO_2 nanofibers, (c) L_2SnO_2 nanofibers, (d) L_4SnO_2 nanofibers, (e) L_6SnO_2 nanofibers, and (f) the magnified L_4SnO_2 nanofibers. The inserts in (a) and (b) are the corresponding TEM images.

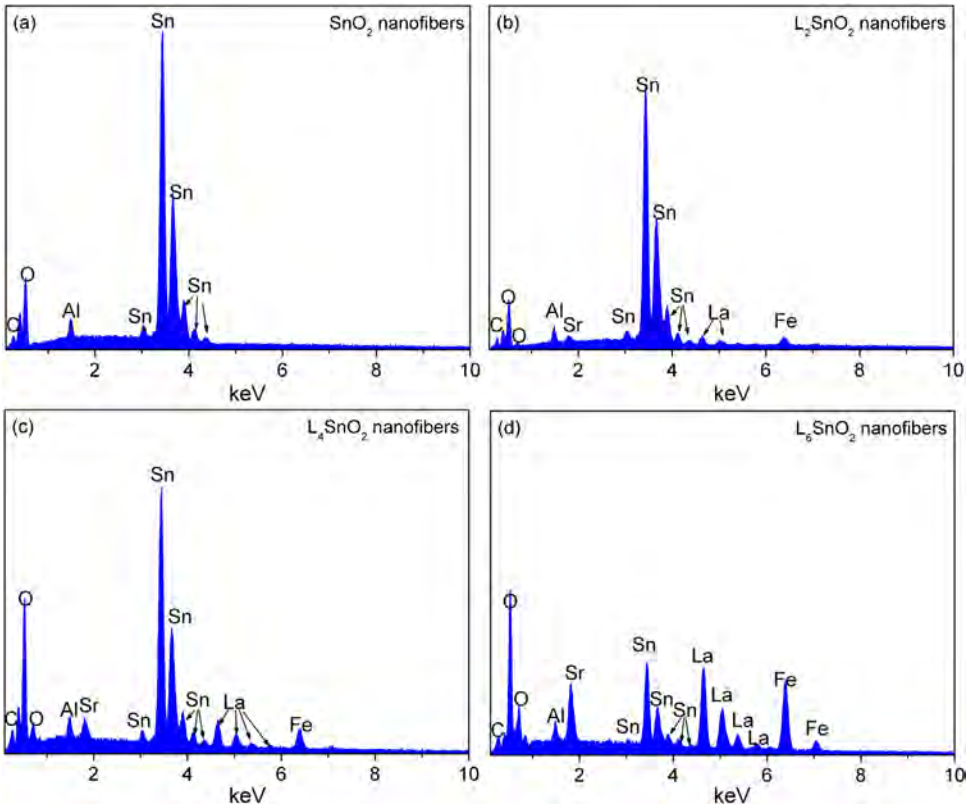

Fig. 5. EDS spectra of (a) SnO_2 nanofibers, (b) L_2SnO_2 nanofibers, (c) L_4SnO_2 nanofibers, and (d) L_6SnO_2 nanofibers.

$La_{0.7}Sr_{0.3}FeO_3$ sensors is 260 °C. In the whole temperature range, the L_2SnO_2 sensors, L_4SnO_2 sensors, and L_6SnO_2 sensors exhibit much higher responses than that of $La_{0.7}Sr_{0.3}FeO_3$ and SnO_2 sensors, indicating the addition of $La_{0.7}Sr_{0.3}FeO_3$ is beneficial to the ethanol sensing of SnO_2 nanofibers. Especially, the L_4SnO_2 sensors show significantly higher response than other samples with the maximum response around 28–1 ppm ethanol at 300 °C. It is more than 5 times larger than that of SnO_2 sensors (about 5) and 8 times larger than that of $La_{0.7}Sr_{0.3}FeO_3$ sensors (about 3).

The response of $La_{0.7}Sr_{0.3}FeO_3$ sensors, SnO_2 sensors, L_2SnO_2 sensors, L_4SnO_2 sensors, and L_6SnO_2 sensors versus ethanol concentration at 300 °C is shown in Fig. 7. The responses increased greatly for ethanol sensing in a lower concentration range of 0.1–10 ppm, and then increased slowly in 10–10,000 ppm, which indicates the sensors become more or less saturated after 10 ppm. Moreover, the L_4SnO_2 sensors show the highest responses than all other samples in the whole concentration range, which further indicates $La_{0.7}Sr_{0.3}FeO_3$-coating is beneficial to the ethanol sensing of SnO_2 nanofibers.

For a gas sensor, quick response and recovery is of great importance. Fig. 8 shows the response and recovery characteristics of the L_4SnO_2 sensors to 1 ppm ethanol at 300 °C. When ethanol was injected into the testing chamber the response of the sensor increased rapidly, when subjected to air the sensor recovered to the initial state quickly. The response and recovery times are calculated to be about 9 s and 15 s, respectively.

Selectivity is another important parameter to evaluate the sensing performance of semiconductor materials. The cross-responses

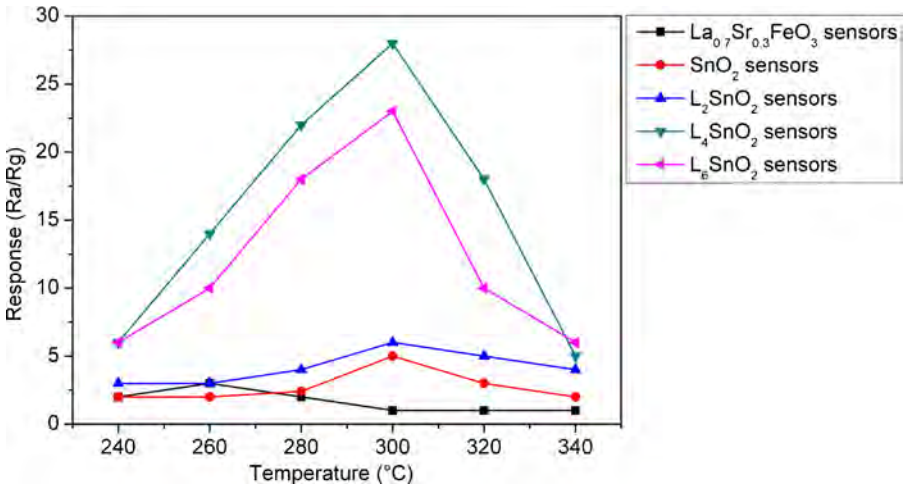

Fig. 6. Responses of $La_{0.7}Sr_{0.3}FeO_3$ sensors, SnO_2 sensors, L_2SnO_2 sensors, L_4SnO_2 sensors, and L_6SnO_2 sensors to 1 ppm ethanol at different operating temperatures.

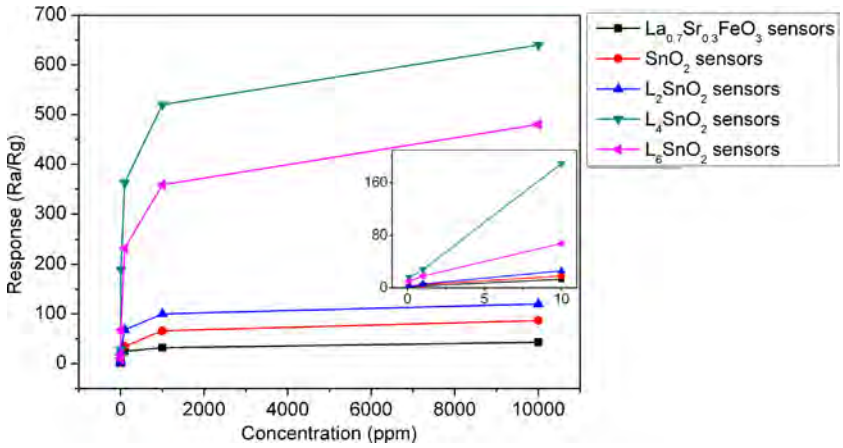

Fig. 7. Responses of $La_{0.7}Sr_{0.3}FeO_3$ sensors, SnO_2 sensors, L_2SnO_2 sensors, L_4SnO_2 sensors, and L_6SnO_2 sensors to different concentrations of ethanol at 300 °C.

of the L_4SnO_2 nanofibers to some typical interference gases such as CH_3COCH_3, NH_3, H_2, C_2H_2, C_6H_6, H_2S, CH_4, and CO (the concentration of all these gases is 1 ppm) were studied at 300 °C (Fig. 9). The L_4SnO_2 sensor exhibits the highest responses to ethanol in the tests, which is due to the suitable operating temperature for SnO_2 to ethanol. Normally, 300 °C is the best operating temperature for SnO_2-based ethanol sensors [9–11]. Both the SnO_2 nanofibers and $La_{0.7}S_{r0.3}FeO_3$ nanoparticles are ethanol sensing materials, the high selectivity of the composite can be expected [15].

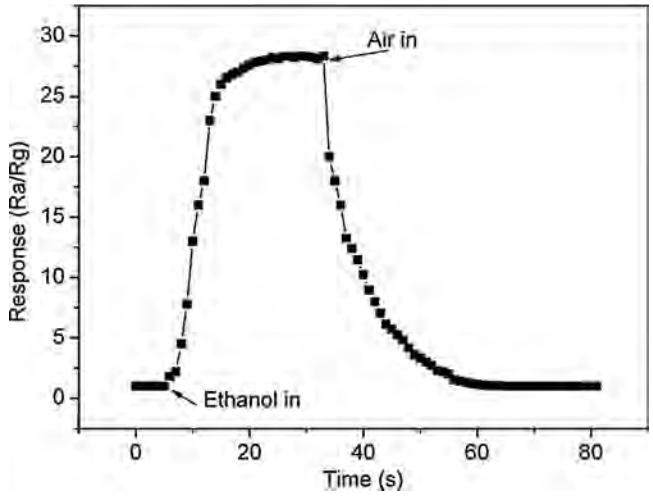

Fig. 8. Response and recovery behavior of L_4SnO_2 sensors to 1 ppm ethanol at 300 °C.

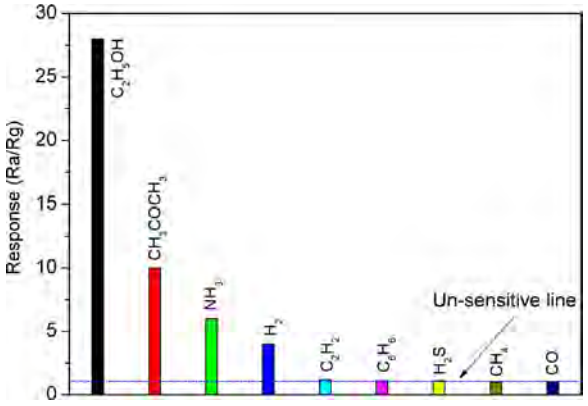

Fig. 9. Cross-responses of the L_4SnO_2 sensors to 1 ppm different gases at 300 °C.

The humidity interference is another important parameter for chemical sensors. Some SnO_2-based sensors are reported to be insensitive at high RH conditions [33]. The L_4SnO_2 sensors were also tested to 1 ppm ethanol at various RHs at 300 °C, as shown in Fig. 10 [34]. The responses only decreased to 16 and 10 at 40% and 65% RHs, respectively. This is achieved by the anti-humidity properties of $La_{0.7}Sr_{0.3}FeO_3$ nanoparticles. $La_{0.7}Sr_{0.3}FeO_3$ nanoparticles can prevent the immersion of water molecules [23], and therefore enhance the sensor response at high humidity conditions.

The long-term stability of the sensor has also been investigated. It is clearly shown in Fig. 11 that the sensor responses are nearly the same during the test. Therefore, the L_4SnO_2 sensors are rather stable.

The sensing mechanism can be explained as follows [35,36]. The response of semiconducting metal oxides is based on the reactions between gas molecules to be detected and the oxygen species absorbed on the surface of metal oxides. Oxygen molecules, which are chemisorbed on SnO_2 nanofibers, can generate several kinds of oxygen species (O^- is believed to be the dominant [37]) and decrease the conductivity of sensor. When ethanol is introduced at a suitable temperature, oxygen species can react with ethanol molecules and release the trapped electron back to the conduction band and result in a reducing of sensor resistance. The reaction between surface absorbed oxygen species and ethanol can be simply described as [24]:

$$C_2H_5OH + 6O^- = 3H_2O + 2CO_2 + 6e^- \quad (1)$$

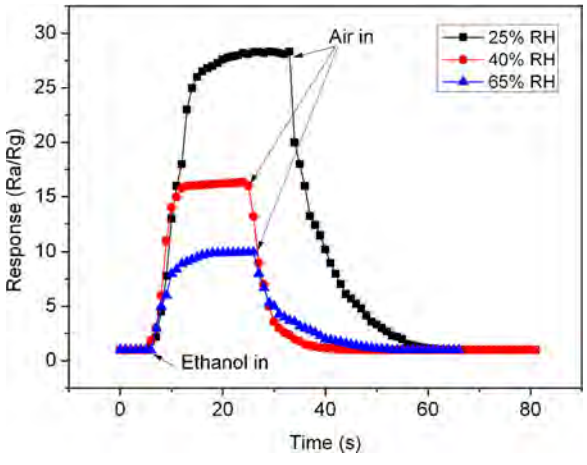

Fig. 10. Response and recovery behavior of L_4SnO_2 sensors to 1 ppm ethanol at various humidity conditions.

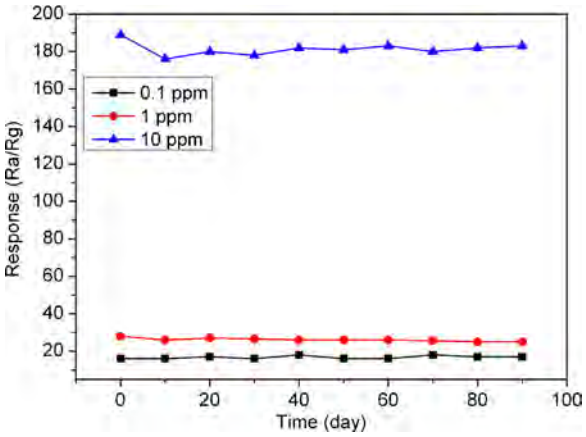

Fig. 11. Stability of the L_4SnO_2 sensor after exposing in air for 90 days.

For the coated nanofibers, the high performance can be ascribed to the following two reasons: (1) the formation of p–n contacts between $La_{0.7}Sr_{0.3}FeO_3$ and SnO_2 can form hetero interfaces with high barrier heights [21]. These hetero interfaces are responsible for the sensor response and selectivity. Two most probable paths of the charge carriers, n–n connection (SnO_2–SnO_2) and p–n ($La_{0.7}Sr_{0.3}FeO_3$-SnO_2) connection, are formed in the interfaces [38]. With suitable coating ratios, the current flow across the p–n interface controls the overall current. When the vicinities of n–p contacting points are exposed to reducing gases at optimize temperatures, the gas molecules can permeate into the interfaces. Changes in electrical properties at the interfaces due to the permeated chemical species are then observed. Various forms of the heterocontact sensors have been reported, including mechanical contact structure [39], thin film structure [39], and composite form [40–43]. However, most of the heteroatoms or heterocontacts are doped both in the interior and on the surface of a semiconducting material. The inside heterocontacts are not only unable to join the sensor reaction, but also rise the sensor resistance for increased barrier heights [22]. p-Type $La_{0.7}Sr_{0.3}FeO_3$ was deposited only on the exterior of n-type SnO_2 nanofibers by this surface-coating method. Thus, the contact efficiency should be much higher than the others. (2) The pore size on the surface of SnO_2 nanofibers is too large and gas molecules can easily overflow the sensing layer through these large pores, which is a disadvantage for sensing reactions [44]. While, these large pores in SnO_2 nanofibers will be filled during coated with $La_{0.7}Sr_{0.3}FeO_3$ nanoparticles, and also more adsorption sites will be provided for both oxygen species and ethanol molecules [45]. It is believed that these two factors are both in favor of the sensing performance of the composites.

4. Conclusions

In summary, coating $La_{0.7}Sr_{0.3}FeO_3$ nanoparticles on the surface of SnO_2 nanofibers can not only form p–n contacts to magnify sensing signals but also provide more absorption sites for the analyzed species. The corresponding sensor shows a high response, which is 28–1 ppm ethanol, and the response and recovery times are about 9 s and 15 s, respectively. It is found that the selectivity and stability of these composite materials are excellent. We believed that it is a possible and effective route for improving the sensing performance of 1D nanostructure by surface doping metal oxide nanoparticles.

Acknowledgements

This work is supported by the National Natural Science Foundation of China (21071060 and 21371070) and the National Basic Research Program of China (973 Program) (2013CB632403).

References

[1] J. Hu, Y. Bando, Q. Liu, D. Golberg, Laser-ablation growth and optical properties of wide and long single-crystal SnO_2 ribbons, Advanced Functional Materials 13 (2003) 493–496.
[2] J. Janata, M. Josowicz, D.M. Devaney, Chemical sensors, Analytical Chemistry 66 (1994) 207–228.
[3] A. Kolmakov, M. Moskovits, Chemical sensing and catalysis by one-dimensional metal-oxide nanostructures, Annual Review of Materials Research 34 (2004) 151–180.
[4] A. Forleo, L. Francioso, S. Capone, F. Casino, P. Siciliano, O.K. Tan, H. Hui, Fabrication at wafer level of miniaturized gas sensors based on SnO_2 nanorods deposited by PECVD and gas sensing characteristics, Sensors and Actuators B: Chemical 154 (2011) 283–287.
[5] B.Y. Wei, M.C. Hsu, P.G. Su, H.M. Lin, R.J. Wu, H.J. Lai, A novel SnO_2 gas sensor doped with carbon nanotubes operating at room temperature, Sensors and Actuators B: Chemical 101 (2004) 81–89.
[6] H.A. Khorami, M. Keyanpour-Rad, M.R. Vaezi, Synthesis of SnO_2/ZnO composite nanofibers by electrospinning method and study of its ethanol sensing properties, Applied Surface Science 257 (2011) 7988–7992.
[7] Z.Y. Cai, J.S. Li, Facile synthesis of single crystalline SnO_2 nanowires, Ceramics International 39 (2013) 377–382.
[8] H. Kim, S. An, C. Jin, C. Lee, Structure and NO_2 gas sensing properties of SnO_2-core/In_2O_3-shell nanobelts, Current Applied Physics 12 (2012) 1125–1130.
[9] X.J. Huang, Y.K. Choi, Chemical sensors based on nanostructured materials, Sensors and Actuators B: Chemical 122 (2007) 659–671.
[10] X. Lu, C. Wang, Y. Wei, One-dimensional composite nanomaterials: synthesis by electrospinning and their applications, Small 5 (2009) 2349–2370.
[11] X. Xie, Z. Shao, Q. Yang, X. Shen, W. Zhu, X. Hong, G. Wang, Controllable synthesis of SnO_2 nanowires and nanobelts by Ga catalysts, Journal of Solid State Chemistry 191 (2012) 46–50.
[12] C. Liewhiran, N. Tamaekong, A. Wisitoraat, A. Tuantranont, S. Phanichaphant, Ultra-sensitive H_2 sensors based on flame-spray-made Pd-loaded SnO_2 sensing films, Sensors and Actuators B: Chemical 176 (2013) 893–905.
[13] A. Chiorino, G. Ghiotti, M.C. Carotta, G. Matinelli, Electrical and spectroscopic characterization of SnO_2 and Pd-SnO_2 thick films studied as CO gas sensors, Sensors and Actuators B: Chemical 47 (1998) 205–212.
[14] C. Fu, J. Wang, M. Yang, X. Su, J. Xu, B. Jiang, Effect of La doping on microstructure of SnO_2 nanopowders prepared by co-precipitation method, Journal of Non-Crystalline Solids 357 (2011) 1172–1176.
[15] M.E. Franke, T.J. Koplin, U. Simon, Metal and metal oxide nanoparticles in chemiresistors: does the nanoscale matter? Small 2 (2006) 36–50.
[16] J.H. Yu, G.M. Cho, Selective CO gas detection of CuO- and ZnO-doped SnO_2 gas sensor, Sensors and Actuators B: Chemical 75 (2001) 56–61.
[17] H. Liu, S. Wu, S. Gong, J. Zhao, J. Liu, D. Zhou, Nanocrystalline In_2O_3–SnO_2 thick films for low-temperature hydrogen sulfide detection, Ceramics International 37 (2011) 1889–1894.
[18] A. Kusior, J. Klich-Kafel, A. Trenczek-Zajac, K. Swierczek, M. Radecka, K. Zakrewska, TiO_2–SnO_2 nanomaterials for gas sensing and photocatalysis, Journal of the European Ceramic Society 33 (2013) 2285–2290.
[19] S. Wang, Y. Xiao, D. Shi, H.K. Liu, S.X. Dou, Fast response detection of H_2S by CuO-doped SnO_2 films prepared by electrodeposition and oxidization at low temperature, Materials Chemistry and Physics 130 (2011) 1325–1328.
[20] Y. Zheng, J. Wang, P. Yao, Formaldehyde sensing properties of electrospun NiO-doped SnO_2 nanofibers, Sensors and Actuators B: Chemical 156 (2011) 723–730.
[21] M. Miyayama, K. Hikita, G. Uozumi, H. Yangida, A.c. impedance analysis of gas-sensing property in CuO/ZnO heterocontacts, Sensors and Actuators B: Chemical 24–25 (1995) 383–387.
[22] S.J. Jung, H. Yanagida, The characterization of a CuO/ZnO heterocontact-type gas sensor having selectivity for CO gas, Sensors and Actuators B: Chemical 37 (1996) 55–60.
[23] Z. Wang, C. Chen, T. Zhang, H. Guo, B. Zou, R. Wang, F. Wu, Humidity sensitive properties of K^+-doped nanocrystalline $LaCo_{0.3}Fe_{0.7}O_3$, Sensors and Actuators B: Chemical 126 (2007) 678–683.
[24] J. Yoo, E.D. Wachsman, NO_2/NO response of Cr_2O_3- and SnO_2-based potentiometric sensors and temperature-programmed reaction evaluation of the sensor elements, Sensors and Actuators B: Chemical 123 (2007) 915–921.
[25] L. Francioso, A. Forleo, S. Capone, M. Epifani, A.M. Taurino, P. Siciliano, Nanostructured In_2O_3–SnO_2 sol–gel thin film as material for NO_2 detection, Sensors and Actuators B: Chemical 114 (2006) 646–655.
[26] J.C. Belmonte, J. Manzano, J. Arbiol, A. Cirera, J. Puigcorbé, A. Vilà, N. Sabaté, I. Gràcia, C. Cané, J.R. Morante, Micromachined twin gas sensor for CO and O_2 quantification based on catalytically modified nano-SnO_2, Sensors and Actuators B: Chemical 114 (2006) 646–655.
[27] S. Royer, A. Van Neste, R. Davidson, S. McIntyre, S. Kaliaguine, Methane oxidation over nanocrystalline $LaCo_{1-x}Fe_xO_3$: resistance to SO_2 poisoning, Industrial & Engineering Chemistry Research 43 (2004) 5670–5680.
[28] D. Li, Y. Xia, Electrospinning of nanofibers: reinventing the wheel? Advanced Materials 16 (2004) 1151–1170.
[29] C. Feng, S. Ruan, J. Li, B. Zou, J. Luo, W. Chen, W. Dong, F. Wu, Ethanol sensing properties of $LaCo_xFe_{1-x}O_3$ nanoparticles: effects of calcination temperature, Co-doping, and carbon nanotube-treatment, Sensors and Actuators B: Chemical 155 (2011) 232–238.
[30] B. Ding, M. Wang, X. Wang, J. Yu, G. Sun, Electrospun nanomaterials for ultrasensitive sensors, Materials Today 13 (2010) 16–27.

[31] K.W. Kim, P.S. Cho, S.J. Kim, J.H. Lee, C.Y. Kang, J.S. Kim, S.J. Yoon, The selective detection of C_2H_5OH using SnO_2–ZnO thin film gas sensors prepared by combinatorial solution deposition, Sensors and Actuators B: Chemical 123 (2007) 318–324.
[32] Z. Wen, Q. Wang, Q. Zhang, J. Li, In situ growth of mesoporous SnO_2 on multiwalled carbon nanotubes: a novel composite with porous-tube structure as anode for lithium batteries, Advanced Functional Materials 17 (2007) 2772–2778.
[33] Z. Ling, C. Leach, The effect of relative humidity on the NO_2 sensitivity of a SnO_2/WO_3 heterojunction gas sensor, Sensors and Actuators B: Chemical 102 (2004) 102–106.
[34] Q. Qi, T. Zhang, X. Zheng, H. Fan, L. Liu, R. Wang, Y. Zeng, Electrical response of Sm_2O_3-doped SnO_2 to C_2H_2 and effect of humidity interference, Sensors and Actuators B: Chemical 134 (2008) 36–42.
[35] L. Liu, S. Li, J. Zhuang, L. Wang, J. Zhang, H. Li, Z. Liu, Y. Han, X. Jiang, P. Zhang, Improved selective acetone sensing properties of Co-doped ZnO nanofibers by electrospinning, Sensors and Actuators B: Chemical 155 (2011) 782–788.
[36] M.C. Carotta, A. Cervi, S. Gherardi, V. Guidi, C. Malagu, G. Martinelli, B. Vendemiati, M. Sacerdoti, G. Ghiotti, S. Morandi, S. Lettieri, P. Maddalena, S. Setaro, $(Ti, Sn)O_2$ solid solutions for gas sensing: a systematic approach by different techniques for different calcination temperature and molar composition, Sensors and Actuators B: Chemical 139 (2009) 329–339.
[37] H. Windischmann, P. Mark, A model for the operation of a thin films tin oxide conductance modulation carbon monoxide sensor, Journal of the Electrochemical Society 126 (1979) 627–630.
[38] S. Mridha, D. Basak, Investigation of a p-CuO/n-ZnO thin film heterojunction for H_2 gas-sensor applications, Semiconductor Science Technology 21 (2006) 928–932.
[39] Y. Ushio, M. Miyayama, H. Yanagida, Effect of interface states on gas-sensing properties of a CuO:ZnO thin-film heterojunction, Sensors and Actuators B: Chemical 17 (1994) 221–226.
[40] D.H. Yoon, J.H. Yu, G.M. Choi, CO gas sensing properties of ZnO–CuO composite, Sensors and Actuators B: Chemical 46 (1998) 15–23.
[41] L.J. Zhou, Y.C. Zou, J. Zhao, P.P. Wang, L.L. Feng, L.W. Sun, D.J. Wang, G.D. Li, Sensors and Actuators B: Chemical 188 (2013) 533–539.
[42] Q.H. Xu, D.M. Xu, M.Y. Guan, Y. Guo, Q. Qi, G.D. Li, Sensors and Actuators B: Chemical 177 (2013) 1134–1141.
[43] J. Su, X.X. Zou, Y.C. Zou, G.D. Li, P.P. Wang, J.S. Chen, Inorganic Chemistry 52 (2013) 5924–5930.
[44] Y. Zhang, J. Li, G. An, X. He, Highly porous SnO_2 fibers by electrospinning and oxygen plasma etching and its ethanol-sensing properties, Sensors and Actuators B: Chemical 144 (2010) 43–48.
[45] L. Francioso, M. Russo, A.M. Taurino, P. Siciliano, Micrometric patterning process of sol–gel SnO_2, In_2O_3 and WO_3 thin film for gas sensing applications: towards silicon technology integration, Sensors and Actuators B: Chemical 119 (2006) 159–166.

Biographies

Qi Qi received his PhD degree in the field of microelectronics and solid state electronics in 2010 from Jilin University. Now he is a postdoctoral fellow in College of Chemistry, Jilin University.

Jun Zhao received her B.Sc. chemistry degree from Changchun Institute of Technology in 2006. She is currently undertaking her PhD on the topic of the characterization and gas sensing properties of TiO_2 and ZnO materials.

Rui-Fei Xuan is a master student at College of Materials Science and Engineering, China University of Mining and Technology in China, and he now is studying in State Key Laboratory of Inorganic Synthesis & Preparative Chemistry, Jilin University in China. His research interest is the synthesis of metal oxide materials.

Pei-Pei Wang is a PhD student at State Key Laboratory of Inorganic Synthesis & Preparative Chemistry, Jilin University in China. Now, she is focused in the field of gas sensor.

Liang-Liang Feng is a master student at State Key Laboratory of Inorganic Synthesis & Preparative Chemistry, Jilin University in China. Her research interest is the synthesis of metal oxide mesoporous materials.

Li-Jing Zhou obtained her B.Sc. chemistry degree at Heibei North University in 2009. Presently, she is a PhD student at State Key Laboratory of Inorganic Synthesis & Preparative Chemistry, Jilin University in China. She is now engaged in the synthesis of Cu-based materials and their application as gas sensors.

De-Jun Wang is a full professor of physical chemistry at College of Chemistry, Jilin University in China. He received his B.Sc. (1977), M.Sc. (1983) and PhD (1989) from Jilin University. His interests include photoelectric sensors, photocatalysts and related materials.

Guo-Dong Li is a full professor at State Key Lab of Inorganic Synthesis & Preparative Chemistry, College of Chemistry, Jilin University in China. He received his B.Sc. (1995), M.Sc. (1998) and PhD (2001) from Jilin University. His research interests include chemical sensors, lithium batteries, photocatalysts and other materials.